Front. Environ. Sci. Eng. 2016, 10(1): 11–18
DOI 10.1007/s11783-014-0714-5

RESEARCH ARTICLE

Removing carbonyl sulfide with metal-modified activated carbon

Juan QIU, Ping NING (✉), Xueqian WANG (✉), Kai LI, Wei LIU, Wei CHEN, Langlang WANG

Faculty of Environmental Science and Engineering, Kunming University of Science and Technology, Kunming 650093, China

Abstract A Cu-Co-K/activated carbon (AC) adsorbent has been developed for the removal of carbonyl sulfide (COS). The effects of COS concentration, reaction temperature and relative humidity were closely examined. A breakthrough of 33.23 mg $COS \cdot g^{-1}$ adsorbent at 60°C, under 30% relative humidity and in presence of 1.0% oxygen was exhibited in the Cu-Co-K/AC adsorbent prepared. Competitive adsorption studies for COS in the presence of CS_2, and H_2S were also conducted. TPD analysis was used to identify sulfur-containing products on the carbon surface, and the results indicated that H_2S, COS and SO_2 were all evident in the effluent gas generated from the exhausted Cu-Co-K/AC. Structure of the activated carbon samples has been characterized using nitrogen adsorption, and their surface chemical structures were also determined with X-ray photoelectron spectroscopy (XPS). It turns out that the modification with $Cu(OH)_2CO_3$-CoPcS-KOH can significantly improve the COS removal capacity, forming SO_4^{2-} species simultaneously. Regeneration of the spent activated carbon sorbents by thermal desorption has also been explored.

Keywords carbonyl sulfide, activated carbon, removal, reactive adsorption

1 Introduction

Recently, removing carbonyl sulfide (COS) from chemical feed stocks has started to regain attention [1]. Particularly, as, one of the most abundant organic sulfur compounds, COS is broadly present in natural gas, liquefied petroleum gas, water gas, and coal gas [2–5]. Although the chemical reactivity of COS is fairly low under atmospheric conditions, it was found that COS could substantially contribute to the formation of SO_2, possibly promoting undesired photochemical reactions [1,2,6,7]. In addition, COS not only has harmful effect on natural environment via leading to acid rain, it also can induce serious damage to the general industry [3,8–10]. Specifically, sulfur is a nonspecific catalyst poisoning agent, which can dramatically reduce the catalytic activity of various catalysts [3,11–13]. For instance, in the Fischer-Tropsch process, as little as 4 mg of sulfur on the surface of 1g Fe-Cu-K catalyst decreases the observed activity by about 50% [1].

So far, a number of strategies have been developed to remove COS molecules from gas, including hydrogenation, adsorption, and hydrolysis [12,14,15]. Particularly, removing sulfur contaminants via adsorption seems to be a viable approach to achieve low sulfur level [16].Different types of adsorbents, including the supported metal oxides (in which the support is typically alumina or carbon) [13,16,17], mixed metal oxides, metal ion-exchanged zeolites and activated carbons have been employed to eliminate COS gas. Naturally, due to the low cost, coal-based carbon material is an attractive alternative adsorbent, plus, the adsorption capacity of activated carbon can be substantially enhanced by modifications, such as, impregnating with transition metals [1]. Melanie et al. found that VPR, BPL, and Centaur can effectively adsorb COS, and the corresponding adsorption capacity at 70°F–80°F under 17% relative humidity (RH) is 1.8, 2.1, and 3.5 mg $COS \cdot g^{-1}$ activated carbon [18].

In this work, we aim to develop a novel Cu-Co-K/AC adsorbent for the removal of COS. Using the COS breakthrough curves, we have investigated the effects of several factors on the removal process, such as COS concentration, reaction temperature and relative humidity. Plus, competitive adsorption of COS in the presence of CS_2 and H_2S were also conducted to gain insightful information. Moreover, the overall adsorption performance has been analyzed via measuring the sulfur species removed from the adsorbents loaded with COS gas by the temperature programmed desorption (TPD) method. In

Received November 26, 2012; accepted April 6, 2014

E-mail: ningping_58@163.com, wxqian3000@aliyun.com

addition, regeneration of the activated carbon sorbents by thermal desorption was also explored. Finally, the external surfaces of adsorbents were examined using X-ray photoelectron spectroscopy (XPS).

2 Materials and methods

2.1 Preparation of adsorbents

The activated carbon was prepared from commercial coal-derived carbon (Jiulong Fine Chemical Factory, Chongqing, China), and then it was used as the adsorbent support in this study. Activated carbon samples were washed 3 times with distilled water to remove soluble impurities on the supports, and dried at 110°C for 24 h. Activated carbon samples (5.0±0.1 g) were impregnated with a mixed solution of KOH, sulfonated cobalt phthalocyanine (CoPcS) and $Cu_2CO_3(OH)_2$(10 wt% KOH, 2.0 wt% CoPcS, 1.0 wt% $Cu_2CO_3(OH)_2$, 25 mL) at 20°C. The impregnation reaction mixture was subsequently stirred at the same temperature for 12 h, and the resulting suspension was filtered. The adsorbent collected was first dried at 110°C for 12 h, and then calcined at 350°C for 6 h. These samples were denoted as Cu-Co-K/AC.

2.2 Experimental apparatus

All adsorption experiments were conducted in a quartz columnar reactor (inner diameter 9 mm, length 60 mm), and the total flow rate has been set to 360 mL·min^{-1}, The model flow gas was composed of nitrogen and COS, which were initially mixed evenly in a mixer with micro-oxygen and then introduced into the adsorption bed unit. For breakthrough test, gas stream was maintained dry, with RH < 1%. The concentration of inlet COS varied from 727 to 754 ppm.

In the competitive adsorption studies, CS_2 and H_2S were employed to examine the potential influence of concurrent substances. Specifically, COS and another substance were simultaneously fed into an activated carbon column, and the concentration of COS was determined to be 748 ppm for no concurrent test, but 430 and 1757 ppm for the tests conducted in the presence of CS_2 and H_2S, respectively.

To study the possible impact of relative humidity, water concentration in the feed was regulated by choosing a saturation temperature that affords the desired water vapor pressure with a specific flow rate of the carrier gas. By adjusting the water bath temperature, a wide range of vapor pressure can be readily achieved.

2.3 Measurements of COS, CS_2, H_2S

The content of COS, CS_2, H_2S was measured with a gas chromatography-flame photometry system using the following parameters: N_2 flow rate 40 mL·min^{-1}, column temperature 50 °C, detector temperature 96 °C, and detection limit 0.003 mg·m^{-3}, A GC-14C gas chromatography with flame photometric detector and a polytetrafluoroethylene-packed column (GD-401 support) was employed in this study. The concentrations of COS, CS_2 and H_2S in the gaseous feed and the effluent from the reactor were determined by an online HC-6 sulfur phosphorus microscale analyzer with a FPD detector.

2.4 Breakthrough measurements

The COS breakthrough curves have been established with dynamic tests within the temperature range of 20°C to 60°C under the relative humidity from 0% to 90%. Each sample was packed in a quartz column and exposed to the flow gas containing 754 ppm COS at a rate of 360 mL·min^{-1}. The concentration of COS was subsequently measured with a gas chromatograph system.

The "breakthrough point" is the point at which the COS removal efficiency in the mixtures with CS_2 or H_2S drop to below 90%. After the experiment was completed, the adsorption capacities of COS in the mixtures with CS_2 or H_2S were calculated with the corresponding integral according to Eq. (1) under various breakthrough conditions [19,20].

$$X = \frac{QC_0t - Q\int_0^t C\mathrm{d}t}{m}, \quad (1)$$

Where, X is the adsorption capacity in mg·g^{-1}, Q is the gas flow in m^3·min^{-1}, t is the adsorption time in min, C_0 is the adsorption column entrance mass concentration in mg·m^{-3}, C is the adsorption column outlet mass concentration in mg·m^{-3}, and m is the adsorbent weight in g.

2.5 N_2 adsorption/desorption

A multi-spot nitrogen adsorption meter NOVA2000e (Quantachrome Corp, USA) was used to determine the nitrogen adsorption isotherms at 77.35 K. Adsorption isotherms can be employed to accurately calculate the specific surface area, volume of micropores, total volume of pores, and micropore size distribution.

2.6 XPS measurements

X-ray photoelectron spectroscopy (XPS) was obtained with a Physical Electronics PHI5600 spectrometer. The X-ray source was operated with an Al Kα anode and photo energy hv 1486.6 eV. The core level binding energy of C 1s for carbon at 284.8 eV has been used as the internal reference for calibration.

2.7 Temperature programmed desorption (TPD)

A 30 mL glass pipette was used as the adsorbent column,

which was oriented vertically, and placed in a tube furnace for TPD tests. Quantitative adsorption tests were performed, in which the carbon adsorbent (3.5 g) was allowed to adsorb of COS for 15 to 16 h at 60°C. After the adsorption was completed, a portion of the adsorbent sample (0.025 g), which was loaded with COS from the quantitative adsorption tests was subjected to TPD analysis. The sample temperature was ramped from 20°C to 500°C at a rate of 10°C·min^{-1}, using a programmable tube furnace. N_2 was used as the sweep gas at a flow rate of 45 mL·min^{-1}, and the exit gas was monitored with gas chromatograph (GC) to detect the presence of sulfur compounds.

3 Results and discussion

3.1 Effects of inlet COS concentration

We have carried out a series of experiments to understand how the inlet COS concentration could affect the performance of COS dynamic adsorption for the Cu-Co-K/AC adsorbents. Several COS breakthrough curves have been obtained, as shown in Fig. 1. Notably, it appears that the COS breakthrough time has slightly decreased when the inlet COS concentration was increased from 754 to 1129 ppm, however, the COS breakthrough adsorption capacity slightly has increased from 33.23 to 37.22 mg·g^{-1}. That said, we conclude that increasing the COS inlet concentration could shorten the breakthrough time of COS and eventually increase its breakthrough adsorption capacity.

On the other hand, it was found that the maximum breakthrough adsorption capacity is 37.22 mg·g^{-1} at a feed concentration of 1129 ppm. Theoretically, the driving force for COS diffusing through the micropores to the active sites would be increased with the rise of COS concentration, which should positively affect the initial adsorption. However, when the concentration of COS was increased to1867 ppm, the COS breakthrough adsorption capacity decreased from 37.22 to 30.86 mg·g^{-1}. When the initial adsorption rate was significantly increased with the sharp rise of COS feed concentration, more products were quickly generated from the reaction to fill the micropores, which would increase the COS diffusion resistance through the pore structure, ultimately reducing adsorption capacity. With the same adsorption time, the amount of COS adsorbed should grow with the increase of feed concentration of the adsorbed species. As a matter of fact, when the adsorption time was increased to 210 min, the amount of COS adsorbed for feeding concentration of 754, 1129, and 1867 ppm turn out to be 36.81, 59.43, and 100.57 mg·g^{-1}, respectively.

3.2 Effects of reaction temperature

As shown in Fig. 2, the effect of adsorption temperature on the COS adsorption capacity for Cu-Co-K/AC adsorbents has been closely examined. Temperature is one of the most important factors that can influence the adsorption of COS, and it was found that the adsorption capacity of COS could be enhanced significantly by raising the adsorption temperature. As illustrated in Fig. 2, the COS breakthrough adsorption capacity at the adsorption temperatures of 20°C, 40°C, and 60°C are 5.856, 21.29, 33.23 mg·g^{-1}, respectively. These results indicate that the mechanism of COS adsorption on the Cu-Co-K/AC adsorbents could be a physical and chemical adsorption process. Theoretically, the increase of breakthrough adsorption capacity should be due to the rising rate of chemisorption reaction at high adsorption temperature.

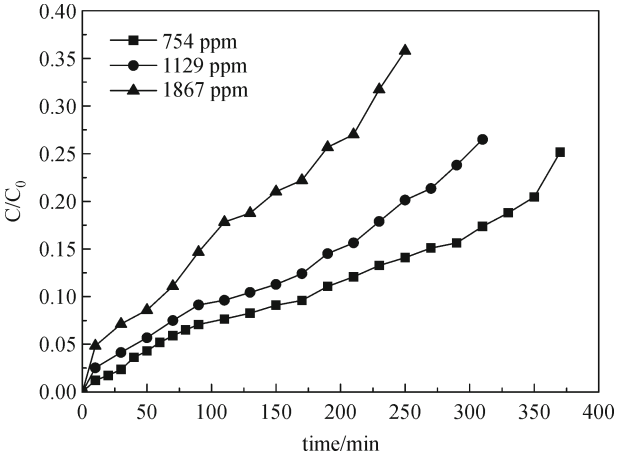

Fig. 1 Effects of COS concentration on COS removal (Reaction condition: 3.5 g sample, 1.0% O_2, 60°C, 30% RH, flow rate 360 mL·min^{-1})

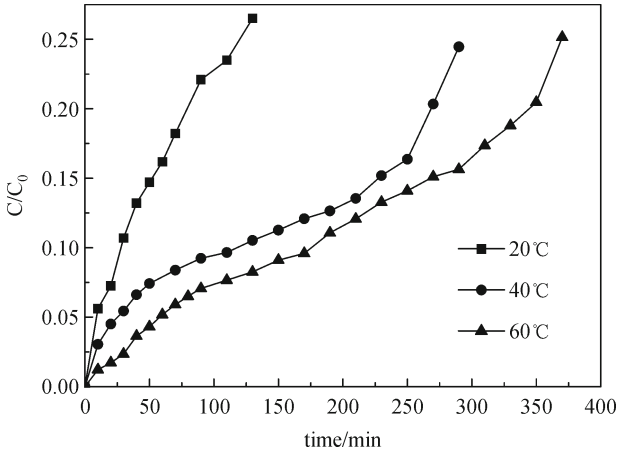

Fig. 2 Effects of reaction temperature on COS removal (Reaction condition: 3.5g sample, COS inlet concentration 754 ppm, 1.0% O_2, 30% RH, flow rate 360 mL·min^{-1})

3.3 Effects of relative humidity

Figure 3 showed the COS breakthrough curves for Cu-Co-K/AC adsorbent in the gas stream with different relative humidity. Notably, it appears that moisture in the gas stream could significantly affected its COS adsorption capability. Indeed, the COS breakthrough capacity for Cu-Co-K/AC adsorbent is 13.65, 33.23, 21.49 and 13.72 $mg \cdot g^{-1}$ under 0%, 30%, 50%, and 90% RH, respectively. These results could be attributed to both physic-sorption and chemi-sorption mechanisms. In this work, it was found that water molecules have adequately improved the COS adsorption capacity, suggesting that certain degree of COS hydrolysis should be occurring. Interestingly, the adsorption capacity seems to decrease at a higher water partial pressures, which presumably should be originated from the competitive adsorption between water and COS molecules [20,21].

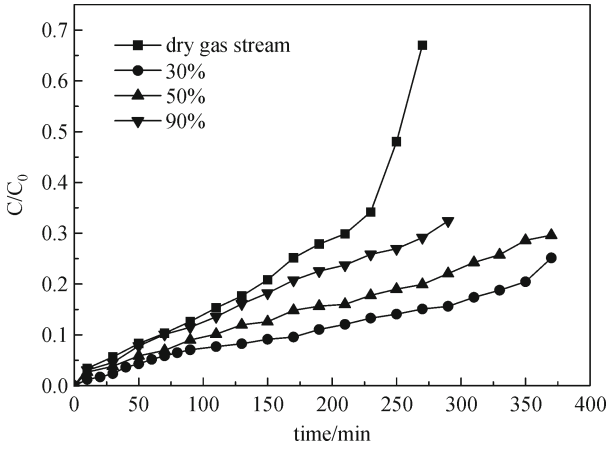

Fig. 3 Effects of relative humidity on COS removal (Reaction condition: 3.5 g sample, COS inlet concentration 754 ppm, 1.0% O_2, 60 °C, flow rate 360 $mL \cdot min^{-1}$)

3.4 Effects of competitive adsorption

Next, we studied the influence of concurrent substances (CS_2 and H_2S) on the breakthrough curves of COS, and the results were summarized in Figs. 4 and 5. Notably, the breakthrough capacity of Cu-Co-K/AC adsorbent for the mixture of COS and CS_2 or H_2S seems to be smaller than the one for sole COS.

Table 1 summarized the breakthrough adsorption capacities for the mixed CS_2 and COS in the gas stream, as well as the results for plain COS at 60°C under 30% RH. The last column on the right showed the percentage of reduction in COS adsorption capacity due to the presence of CS_2. Notably, it appears that the breakthrough adsorption capacity of COS has decreased by 42.55% because of CS_2, which accounts for 37.16% of the pollutant molecules. Compared with COS molecules, approximately 10% of the CS_2 molecules have adsorbed onto the adsorbent. Possibly, adsorbents contain internal pores that smaller COS molecules can fit but CS_2 molecules cannot. Even though some sites are still available for larger CS_2 molecules, COS molecules could effectively competes and retain a significant portion [18,22].

Table 2 showed the breakthrough adsorption capacities for the mixed H_2S and COS in the gas stream, as well as the previous results for plain COS at 60°C under 30% RH. As illustrated in Table 2, the reduction of COS adsorption capacity in the presence of H_2S is 41.44% and H_2S accounts for 70.29% of the pollutant molecules. In addition, it appears that each adsorbent can retain H_2S approximately nine times of COS. Therefore, we conclude that a huge amount of additional sites should be available to H_2S adsorption, and the adsorbent prepared could contain internal pores accessible to small H_2S, but not to COS. For the sites that are available to the large COS molecules, H_2S molecules still can effectively compete and ultimately retain a large portion. Interestingly, it appears that the amount of COS adsorbed was actually reduced, which could be due to the lower polarity of COS molecules. To the contrast, a wider range of surface sites are available to the more polar H_2S molecules for adsorption [18,22].

3.5 Temperature programmed desorption analysis

Temperature programmed desorption (TPD) analysis has been used to understand the role of Cu-Co-K/AC in the improvement of COS capacity and valuable information about the possible adsorption mechanism of COS on the

Table 1 COS and CS_2 breakthrough adsorption capacities, at 60°C under 30% RH

samples	inlet COS	inlet CS_2	% of pollutant molecules that are CS_2	breakthrough adsorption capacity			% reduction in COS adsorption capacity because of CS_2
				CS_2 in presence of COS	COS in presence of CS_2	COS by itself	
Cu-Co-K/AC	727.8 ppm	430.3 ppm	37.16	2.873 $mg \cdot g^{-1}$	19.09 $mg \cdot g^{-1}$	33.23 $mg \cdot g^{-1}$	42.55
				0.0378 $mmol \cdot g^{-1}$	0.3182 $mmol \cdot g^{-1}$	0.5538 $mmol \cdot g^{-1}$	ratio of moles CS_2 to moles COS adsorbed
							0.1188

Table 2 COS and H_2S breakthrough adsorption capacities, at 60 °C under 30% RH

samples	inlet COS	inlet H_2S	% of pollutant molecules that are H_2S	breakthrough adsorption capacity			% reduction in COS adsorption capacity because of H_2S
				H_2S in presence of COS	COS in presence of H_2S	COS by itself	
Cu-Co-K/AC	742.8 ppm	1757 ppm	70.29	100.53 mg·g^{-1}	19.46 mg·g^{-1}	33.23 mg·g^{-1}	41.44
				2.952 mmol·g^{-1}	0.3243 mmol·g^{-1}	0.5538 mmol·g^{-1}	ratio of moles H_2S to moles COS adsorbed
							9.103

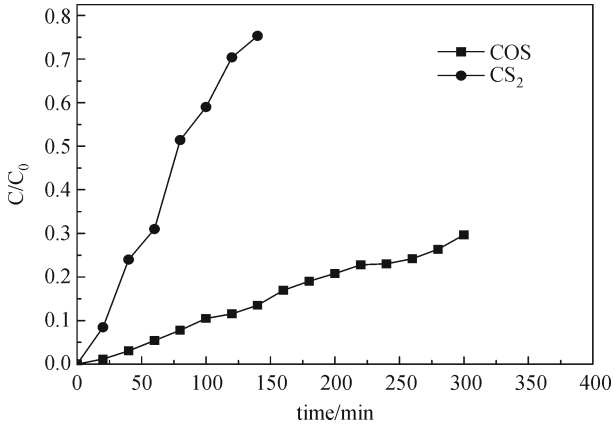

Fig. 4 Effect of CS_2 competitive adsorption on COS removal

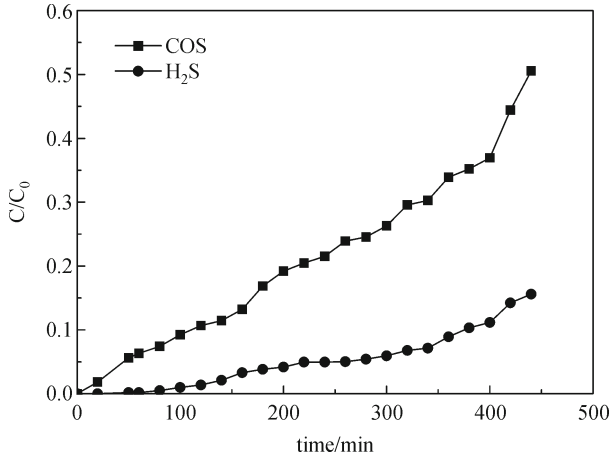

Fig. 5 Effect of H_2S competitive adsorption on COS removal

carbon surface could also be obtained [23]. The relationship between the concentrations of sulfur-containing compounds in the off gas and desorption temperatures has been illustrated in Fig. 6. H_2S, COS and SO_2 molecules have been detected in the effluent gas generated from the exhausted Cu-Co-K/AC adsorbents during the TPD process. Notably, H_2S was first detected at 60°C and its content reached the maximum at 300°C. Plus, it appears that desorption process is fully completed at 500°C. Both COS and SO_2 molecules have been detected in the effluent gas, accompanying H_2S.

Theoretically, COS molecules can be adsorbed onto the activated carbon surface and then hydrolyzed by functional groups, water vapor, or adsorbed oxygen. H_2S and COS are the primary sulfur compounds detected at the exit of the TPD process for the exhausted Cu-Co-K/AC with a small amount of SO_2. These results suggest that the adsorption, hydrolysis and oxidation of COS molecules could occur on the carbon surface, resulting in the production of H_2S, COS and SO_2.On the other hand, it was found that a large amount of H_2S was released from the exhausted Cu-Co-K/AC tests, indicating that Cu-Co-K could serve as a catalyst for such reactions. These results also suggest that a part of COS could be adsorbed on the adsorbent by physical adsorption, whereas the rest should be first hydrolyzed and then adsorbed on the adsorbent.

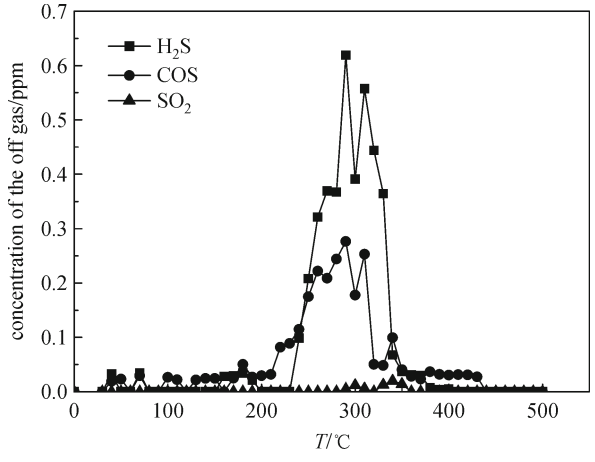

Fig. 6 TPD profiles from the analyses of the N_2 sweep gas at the exit of the test apparatus during the thermal desorption of COS adsorbed Cu-Co-K/AC

3.6 Effects on pore structure

We next examined the different pore size distribution of AC, Cu-Co-K/AC, and Cu-Co-K/AC-E (the sample after the COS adsorption) material, and the results were illustrated in Fig. 7. In addition, the BET surface area, average pore radius, micro-and total pore volumes for these three samples were summarized in Table 3.

As shown in Fig. 7, for most of the samples, their pore volumes are well below 2 nm. Particularly, modification

Table 3 Porosity parameters for activated carbon samples

samples	$S_{BET}/(m^2 \cdot g^{-1})$	$V_{micro}/(cm^3 \cdot g^{-1})$	$V_{total}/(cm^3 \cdot g^{-1})$	$D_{average}$ /nm
AC	829.7	0.4400	0.4898	1.181
Cu-Co-K/AC	536.4	0.3030	0.3369	1.256
Cu-Co-K/AC-E	485.6	0.2550	0.2841	1.170

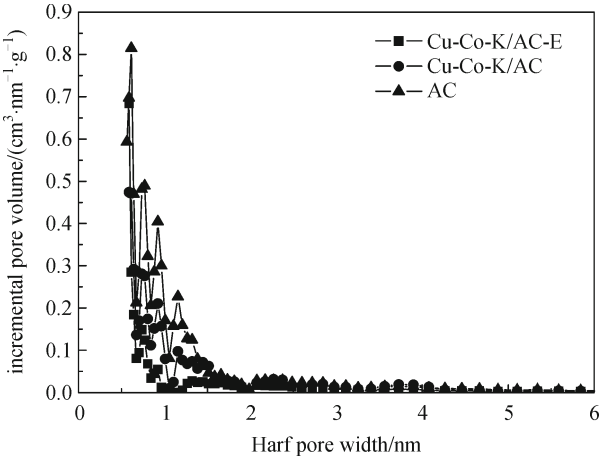

Fig. 7 Comparison of the pore size distributions of Cu $(OH)_2CO_3$-CoPcS-KOH modified samples before and after the COS adsorption

with $Cu(OH)_2CO_3$-CoPcS-KOH has resulted in the decrease of the volume of pores to less than 2 nm, especially for samples with micropore volume of pores with sizes ranging from 0.7 to 1.5 nm. Apparently, Cu $(OH)_2CO_3$-CoPcS-KOH is an effective modification agent affording pore blockage in the micropores which were caused by the groups grafted on during the impregnation process. Moreover, further exposure to COS would result in a more visible decrease in the micropores of the samples.

Using the linear part of the nitrogen adsorption isotherms, the specific surface area of each sample (S_{BET}) can be calculated according to the Brunauer, Emmett, and Teller method, as shown in Table 3. In addition, pore structure parameters such as micro-pore volume, pore volume, and average pore size can also be obtained based on the Density Function Theory (DFT). A comparison between AC and Cu-Co-K/AC showed that the impregnation process has led to a volume decrease, particularly for those with volume of pores smaller than 2 nm, which account for 89.6% of the total pore volume reduction. Notably, it appears that the $Cu(OH)_2CO_3$-CoPcS-KOH modification has decreased surface areas and micropore volume by 35.35% and 31.14%, respectively. Results obtained from the pore size distribution also indicate that all micropores have been adequately impacted by the impregnation process.

A broad comparison between Cu-Co-K/AC and Cu-Co-K/AC-E has been conducted, and the results were summarized in Fig. 7 and Table 3. Specifically, significant changes are evident in the adsorbent voidage for both material, presumably due to the COS adsorption. Plus, their surface areas have decreased 9.48% and 8.62%, which should be originated from the decrease of micropore volumes.

Thus, it appears that the activated carbon activity in the COS chemical adsorption process is distinctively different, which essentially suggests that the $Cu(OH)_2CO_3$-CoPcS-KOH compound loaded in the micropores should play a catalytic role in the overall COS reactive adsorption process.

3.7 X-ray photoelectron spectroscopic analysis

XPS analysis was performed to determine the composition of S element in the used catalyst and its valence states, and the details of S 2p XPS spectra of the used adsorbent were shown in Fig. 8. Obviously, the peaks in the curves are corresponding to the S 2p signal at 168.69 eV and 170.08 eV, suggesting the presence of SO_4^{2-} ions on the adsorbent surface. Theoretically, these SO_4^{2-} species observed in the exhausted Cu-Co-K/AC could be originated from the oxidation process [24,25].

Therefore, we conclude that $Cu(OH)_2CO_3$-CoPcS-KOH plays important roles in the reaction process in which the activated carbon adsorbs COS, as well as the reactive adsorption process in which COS molecules are attached onto the surface of the activated carbon.

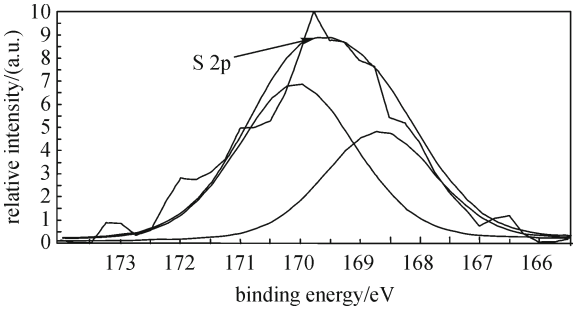

Fig. 8 Detail S 2p XPS spectral of exhausted Cu-Co-K/AC samples

3.8 Thermal regeneration

Temperature programmed desorption (TPD) is a viable approach for the regeneration of spent adsorbents, as demonstrated in the literature reports [23]. Several Cu-Co-

K/AC adsorbents were first used in the COS breakthrough test, and then underwent TPD regeneration process. The resulting material was subject to COS breakthrough analysis and the results were summarized in Fig. 9 (sample referred to as Cu-Co-K/AC-R1, Cu-Co-K/AC-R2, and Cu-Co-K/AC-R3). Compared with fresh Cu-Co-K/AC adsorbent, the regenerated materials have exhibited similar adsorption behaviors (Cu-Co-K/AC-R1and Cu-Co-K/AC-R2). However, a shorter breakthrough time has been observed for Cu-Co-K/AC-R3, which is different from Cu-Co-K/AC-R1 and Cu-Co-K/AC-R2. Therefore, we conclude that the spent Cu-Co-K/AC could be effectively regenerated by thermal desorption process, and capacity loss or decrease of the surface area and volume of micropores should be marginal.

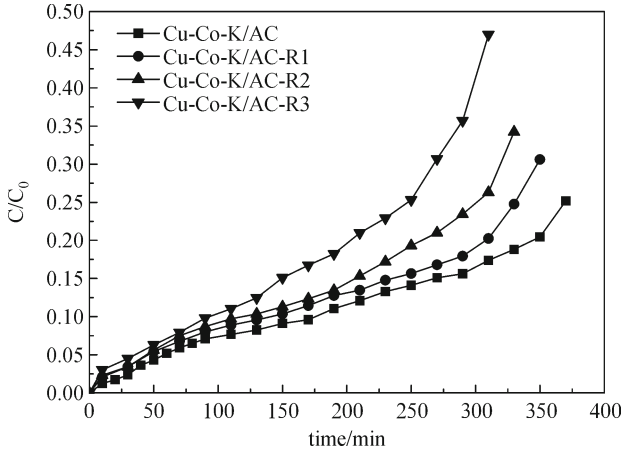

Fig. 9 Breakthrough curves of fresh and regenerated Cu-Co-K/AC sorbent samples. Regenerated samples are referred to as Cu-Co-K/AC-R#, where # indicates the number of times the sample has been regenerated

4 Conclusions

In conclusion, we have developed an efficient Cu-Co-K/AC adsorbent for the removal of COS under low temperature conditions. Particularly, the breakthrough tests have demonstrated that the removal time and capacities for such Cu-Co-K/AC material are superior. As expected, it appears that both temperature and relative humidity play critical roles in the COS removing process. Notably, samples prepared in our laboratory have exhibited a breakthrough capacity of 33.23 mg $COS \cdot g^{-1}$ adsorbent at 60 °C under 30% RH in the presence of 1.0% oxygen. Moreover, the COS adsorption capacity in the presence of CS_2, H_2S was reduced by 42.55% and 41.44%, respectively. H_2S, COS and SO_2 are found to be the primary products in the effluent gas generated from the exhausted Cu-Co-K during the TPD process.

It is highly possible that the $Cu(OH)_2CO_3$-CoPcS-KOH impregnation could lead to the formation of surface functional groups. Even all micropores could be affected by the impregnation process; this work showed that pores smaller than 2 nm should be the main source for the reduction of total pore volume of adsorbent.

Subsequent XPS analysis indicated that the sulfur species adsorbed on the Cu-Co-K/AC material should be in the state of SO_4^{2-}. The $Cu_2(OH)_2CO_3$-CoPcS-KOH species in the micropores can also function as the catalyst for the reactive adsorption process on the surface of the impregnated samples. Therefore, we conclude that such $Cu_2(OH)_2CO_3$-CoPcS-KOH impregnated activated carbon should be promising adsorbent material for removing COS from gas streams.

Acknowledgements This work was supported by the National Natural Science Foundation of China (Grant Nos. U1137603, 51268021 and 51368026), the National High Technology Research and Development Program of China (No. 2012AA062504) and the Applied Basic Research Program of Yunnan (Nos. 2011FB027 and 2011FA010).

Reference

1. Rhodes C, Riddel S A, West J, Williams B P, Hutchings G J. The low-temperature hydrolysis of carbonyl sulfide and carbon disulfide: a review. Catalysis Today, 2000, 59(3–4): 443–464
2. Wang H Y, Yi H H, Ning P, Tang X L, Yu L L, He D, Zhao S. Calcined hydrotalcite-like compounds as catalysts for hydrolysis carbonyl sulfide at low temperature. Chemical Engineering Journal, 2011, 166(1): 99–104
3. Williams B P, Young N C, West J, Rhodes C, Hutchings G J. Carbonyl sulphide hydrolysis using alumina catalysts. Catalysis Today, 1999, 49(1–3): 99–104
4. Svoronos P D N, Bruno T J. Carbonyl sulfide: a review of its chemistry and properties. Industrial & Engineering Chemistry Research, 2002, 41(22): 5321–5336
5. Hinderaker G, Sandal O C. Absorption of carbonyl sulfide in aqueous diethanolamine. Chemical Engineering Science, 2000, 55 (23): 5813–5818
6. Wang L, Wang S D, Yuan Q, Lu G Z. COS hydrolysis in the presence of oxygen: Experiment and modeling. Journal of Natural Gas Chemistry, 2008, 17(1): 93–97
7. Liu Y C, He H, Mu Y J. Heterogeneous reactivity of carbonyl sulfide on α-Al_2O_3 and γ-Al_2O_3. Atmospheric Environment, 2008, 42(5): 960–969
8. Zhang Y Q, Xiao Z B, Ma J X. Hydrolysis of carbonyl sulfide over rare earth oxysulfides. Applied Catalysis B: Environmental, 2004, 48(1): 57–63
9. Huang H M, Young N, Williams B P, Taylor S H, Hutchings G. COS hydrolysis using zinc-promoted alumina catalysts. Catalysis Letters, 2005, 104(1–2): 17–21
10. Yi H H, Wang H Y, Tang X L, Ning P, Yu L L, He D, Zhao S Z. Effect of calcination temperature on catalytic hydrolysis of COS over CoNiAl catalysts derived from hydrotalcite precursor. Industrial & Engineering Chemistry Research, 2011, 50(23): 13273–13279

11. Toops T J, Crocker M. New sulfur adsorbents derived from layered double hydroxides II. DRIFTS study of COS and H_2S adsorption. Applied Catalysis B: Environmental, 2008, 82(3–4): 199–207
12. Huang H M, Young N, Williams B P, Taylor S H, Hutchings G. High temperature COS hydrolysis catalysed by γ-Al_2O_3. Catalysis Letters, 2006, 110(3–4): 243–246
13. Jackson S D, Leeming P, Webb G. Supported metal catalysts: Preparation, characterisation, and function IV. Study of hydrogen sulphide and carbonyl sulphide adsorption on platinum catalysts. Journal of Catalysis, 1996, 160(2): 235–243
14. Wang X Z, Ding L, Zhao Z B, Xu W Y, Meng B, Qiu J H. Novel hydrodesulfurization nano-catalysts derived from Co_3O_4 nanocrystals with different shapes. Catalysis Today, 2011, 175(1): 509–514
15. Thomas B, Williams B P, Young N, Rhodes C, Hutchings G J. Ambient temperature hydrolysis of carbonyl sulfide using γ-alumina catalysts: effect of calcination temperature and alkali doping. Catalysis Today, 2003, 86(4): 201–205
16. Sparks D E, Morgan T, Patterson P M, Tackett S A, Morris E, Crocker M. New sulfur adsorbents derived from layered double hydroxides I: Synthesis and COS adsorption. Applied Catalysis B: Environmental, 2008, 82(3–4): 190–198
17. Sakanishi K, Wu Z H, Matsumura A, Saito I, Hanaoka T, Minowa T, Tada M, Iwasaki T. Simultaneous removal of H_2S and COS using activated carbons and their supported catalysts. Catalysis Today, 2005, 104(1): 94–100
18. Sattler M L, Rosenberk R S. Removal of carbonyl sulfide using activated carbon adsorption. Journal of the Air & Waste Management Association, 2006, 56(2): 219–224
19. Wang X, Ning P, Shi Y, Jiang M. Adsorption of low concentration phosphine in yellow phosphorus off-gas by impregnated activated carbon. Journal of Hazardous Materials, 2009, 171(1–3): 588–593
20. Huang C C, Chen C H, Chu S M. Effect of moisture on H_2S adsorption by copper impregnated activated carbon. Journal of Hazardous Materials, 2006, 136(3): 866–873
21. Li J, Li Z, Liu B, Xia Q B, Xi H X. Effect of relative humidity on adsorption of formaldehyde on modified activated carbons. Chinese Journal of Chemical Engineering, 2008, 16(6): 871–875
22. Masuda J J, Fukuyama J J, Fujii S. Influence of concurrent substances on removal of hydrogen sulfide by activated carbon. Chemosphere, 1999, 39(10): 1611–1616
23. Cui H, Turn S Q. Adsorption/desorption of dimethylsulfide on activated carbon modified with iron chloride. Applied Catalysis B: Environmental, 2009, 88(1–2): 25–31
24. Yi H H, He D, Tang X L, Wang H Y, Zhao S Z, Li K. Effects of preparation conditions for active carbon-based catalyst on catalytic hydrolysis of carbon disulfide. Fuel, 2012, 97: 337–343
25. Wang X Q, Qiu J, Ning P, Ren X G, Li Z Y, Yin Z F, Chen W, Liu W. Adsorption/desorption of low concentration of carbonyl sulfide by impregnated activated carbon under micro-oxygen conditions. Journal of Hazardous Materials, 2012, 229–230: 128–136